A Novel Design of Aperiodic Arrays for Ultrawideband Beam Scanning and Full Polarization Reconfiguration

Ziyu Zhang [1], Jia Liu [1], Jianxun Su [1,*], and Jiming Song [2]

[1] State Key Laboratory of Media Convergence and Communication
Communication University of China, Beijing, 100024, China
*sujianxun_jlgx@163.com

[2] Electrical and Computer Engineering
Iowa State University, Ames, IA 50011, USA

Abstract ─ In this letter, a multifunction aperture array is proposed for ultrawideband (UWB) scanning and polarization reconfiguration. The UWB array consisted of linearly polarized elements is capable of operating in four polarization modes (+45° linear polarization (LP), -45° linear polarization, left-hand circular polarization (LHCP) and right-hand circular polarization (RHCP)). This work involves two essential techniques: (a) A new beam-scanning UWB array synthesis approach. An iterative convex optimization strategy is utilized to determine the element locations and obtain the minimum sidelobe level (SLL) for multiple patterns. (b) The polarization reconfigurable technique for beam-scannable arrays. In this part, a sequential rotation and excitation compensation (SR-EC) technique provides polarization reconfiguration for a beam-scannable array consisting of linearly polarized elements. A beam-scanning UWB array is designed by using the proposed UWB array synthesis approach and the SR-EC polarization reconfigurable technique. The Feko numerical result shows 0°-60° beam peak steering, a 4:1 bandwidth (1-4 GHz), and four-polarization reconfigurability.

Index Terms ─ Array synthesis, beam scanning, polarization reconfiguration, ultrawideband.

I. INTRODUCTION

With the development of wireless systems, ultrawideband (UWB) array antennas have attracted significant interests due to their potential of realizing multiple functions within one radiating aperture. In addition to the bandwidth, other requirements are needed to meet in practical multifunction systems, such as wide-angle beam steering, and multi-polarization, etc. It is a challenge to design a single radiating aperture that fulfills all the requirements.

In the literature, many methods have been proposed to develop a wideband array antenna with beam scanning. One way is to use a tightly coupled array antenna to provide ultrawideband (UWB) characteristics and beam scanning, such as in [1-4]. Although tightly coupled array antennas have many advantages, such as high aperture efficiency and wide-angle beam scanning, some drawbacks, such as sophisticated design techniques and high system cost, are also inevitable. Another way of designing UWB array antennas is to adopt nonuniformly spaced techniques. In [5-6], the stochastic optimization algorithms are used to design array antennas. In [7-8], a general SA design approach has been proposed based on polynomial model of an array. An l_0-norm constrained normalized least-mean-square adaptive beamforming algorithm for controllable sparse antenna arrays was presented in [9]. Many studies have been done to develop aperiodic array configurations. However, most aperiodic array synthesis methods focus on the problem of suppressing the grating-lobe and sidelobe levels (SLLs) at a single frequency. In [10], by virtue of the concept of design frequency, the proposed method transforms the beam-scannable UWB design to a problem of synthesizing a broadside fixed-beam array at a single frequency. In [11], the SLL is optimized at the highest operating frequency of the designed array. In the above method, although the sidelobe level is lower at the frequency, it will be uncontrolled at other frequencies. Thus, choosing the best common element positions for meeting lower SLL in the whole frequency band of interest is challenging. A novel array synthesis approach is proposed to achieve it. The optimization method realizes accurate control of the SLL for multiple patterns and guarantees the minimum element spacing in the optimization process. For the multiple constraint problem, an iterative convex optimization strategy is utilized to solve the problem. Specific principles will be introduced in Section II.

In recent years, many polarization reconfigurable antennas have been proposed [12-16]. However, few researches have been done on polarization reconfigurable and UWB beam-steering antenna arrays. An antenna

array that provides wideband frequency agility with simultaneous polarization reconfiguration is presented in [17]. The antenna has the ability of ±28° beam peak steering at 2.4 GHz for both the linear and circular polarizations. The bandwidth and scanning range are narrow.

This paper presents an ultrawideband and polarization reconfigurable electric scanning array, which is constructed by sequential rotating linearly polarized elements. The sequential rotation and excitation compensation (SR-EC) technique is an attractive approach to retain multiple polarization purity for beam-scannable arrays. The specific method will be discussed in Section III. And, the simulated results are given in Section IV.

II. A NOVEL BEAM-SCANNING UWB ARRAY SYNTHESIS APPROACH

For a linear array consisting of N elements whose elements are located at $[x_0, x_1, \ldots, x_{N-1}]$ along with x-axis. Assume that this array works at the frequency f, with a focused beam scanned in θ_o. The array factor can be expressed as the following:

$$AF(\beta, u) = \sum_{n=0}^{N-1} \exp(j\beta x_n u), \qquad (1)$$

where $\beta = 2\pi f/c$, $u = \sin\theta - \sin\theta_o$, and $\theta \in [-\pi/2, \pi/2]$ is the wave propagation direction measured from the z-axis. For a beam-scanning UWB array, the highest and lowest frequency is f_H and f_L, with a focused beam scanned within the range of $[-\theta_{max}, \theta_{max}]$. From (1), the beam-scannable UWB array factor has the following property:

$$\left\{ AF([\beta], [u]) \right\} = \sum_{n=0}^{N-1} \exp(j\beta x_n u), \qquad (2)$$

where $\{AF([\beta], [u])\}$ denote the range of the function $AF(\beta, u)$ varying with $\beta \in [\beta_L, \beta_H]$ and $u \in [-1 - \sin\theta_{max}, 1 + \sin\theta_{max}]$, $\beta_L = 2\pi f_L/c$, $\beta_H = 2\pi f_H/c$. This means that the design of a beam-scannable UWB array can be equivalent to a design of fixed equation. In general, one should check the scannable beam performance in the whole frequency band of interest for the beam-scannable UWB array design problem. The increased computational and storage loads is necessary to deal with requirements of multiple beam scanning angles at multiple frequencies for the beam-scannable UWB array design.

$\{AF([\beta], [u])\}$ indicates the array factor which included all the beam characteristics of the UWB array in the whole frequency band $[f_L, f_H]$ for all beam scanning cases for $\theta_o \in [-\theta_{max}, \theta_{max}]$. Thus, we can consider designing the array factor $\{AF([\beta], [u])\}$ to check all the beam performance of a scannable UWB array. For most of UWB array synthesis cases, the element spacing and the element count N can be determined by considering the antenna element structure and gain requirement in

applications.

In order to achieve better UWB array performance, an iterative convex optimization strategy is developed to successively optimize the UWB array SLL. The basic idea is introducing the elememt spacing variables d_m ($m = 1, \ldots, N\text{-}1$) to the original positions x_n ($n = 0, 1, \ldots, N\text{-}1$) and then find a way to obtain the optimal d_m. The element position and the element spacing can be shown as:

$$\begin{cases} x_0 = 0 \\ x_n = \sum_{m=1}^{n} d_m \ (n = 1, 2, \cdots, N\text{-}1) \end{cases} \cdot \qquad (3)$$

Consider the array factor $\{AF([\beta], [u])\}$ associated with varying positions x_n ($n = 0, 1, \ldots, N\text{-}1$). That is given by

$$\left\{ AF([\beta], [u]) \right\} = 1 + \sum_{n=1}^{N-1} \exp\left(j\beta \sum_{m=1}^{n} d_m u\right). \qquad (4)$$

Now the variables d_m can be optimized by using convex optimization to reduce the overall SLL. However, for a practical UWB array design problem, the following two kinds of constraints should be considered. Typically, the minimum element spacing should be constrained to avoid strong mutual coupling, which can have a detrimental effect on the driving port impedances. In addition, the array aperture size is very significant in practical applications. Thus, the maximum element spacing should also be constrained:

$$a \le d_m \le b \quad m = 1, 2, \cdots N\text{-}1 , \qquad (5)$$

where, a is the minimum element spacing, and b is the maximum element spacing. The optimal element spacing variables can be found by solving the following constrained optimization problem:

$$\min \varepsilon$$
$$\text{s.t.} \begin{cases} \max\left(1 + \sum_{n=1}^{N-1} \exp\left(j\beta \sum_{m=1}^{n} d_m u_o\right)\right) \le \varepsilon \\ u_o \in U_{sl} \\ \beta \in [\beta_L, \beta_H] \\ a \le d_m \le b \quad m = 1, 2, \cdots, N\text{-}1 \end{cases}, \qquad (6)$$

where U_{sl} denotes the sidelobe region in u_o-space. Clearly, the above problem can be efficiently solved by using the iterative convex optimization strategy. Each iteration finds locally optimal element spacing and thus the element spacing can be successively updated until the obtained SLL maintains the same for many times. Besides, it should be mentioned that all the excitation amplitudes remain one in the element spacing optimization process.

The proposed beam-scannable UWB array design procedure is given in Algorithm 1. In this procedure, the

initial element spacing is randomly generated. Then a number of constrained convex optimizations given in (6) are performed to successively update the element spacing, such that the obtained maximum SLL can be reduced as much as possible.

Algorithm 1:

1: Set the frequency band $[f_L, f_H]$, beam scanning range $[-\theta_{max}, \theta_{max}]$, and element number parameter N.

2: Depending on the application requirement, set the range of element spacing $[a, b]$.

3: Set k = 0. Sample the space of u_o, frequency band, and beam scanning range, and initialize element spacings d_m (m = 1,2, . . . , N-1).

4: k = k + 1.

5: Solve the constrained convex optimization problem (6) to find the better element spacings d_m for m = 1, 2, . . . , N-1.

6: Update the element spacings, compute the pattern $\{AF([\beta], [u_o])\}$ in (4) with the new element spacings and obtain the maximum SLL ε.

7: Repeat Steps 4 to 6 until ε remains the same for multiple times or k reaches the allowable maximum number of iterations.

8: Output the obtained element spacings d_m for m = 1,2, . . . , N-1 and calculate the beam-scannable wideband pattern $\{AF([\beta],[u])\}$ in (4).

We consider synthesizing a UWB array consisted 51-element (N=51) occupying the frequency band from 1 to 4 GHz with beam scanning from 0° to 60°. That is $[\beta] = [2\pi f_L/c, ..., 2\pi f_H/c]$, $[\theta_o] = [\ 0°, ..., 60°]$. Set $[\theta] = [\ -90°, ..., 90°]$. Then $[u] = [u_{min}, ..., u_{max}]$, where $u_{min} = -1 - \sqrt{3}/2$, $u_{min} = 1$. We set the minimum element spacing is $\lambda_L/2$ and the maximum element spacing is λ_L, where λ_L is the wavelength at the lowest frequency. Set the initial element spacings $d = [\lambda_L/2, \lambda_L/2, ..., \lambda_L/2]$.

The antenna pattern is calculated according to (4) and the above data. The pattern contains both operating frequencies and beam-scanning information. Extract the maximum value SLLmax from the sidelobe information of the pattern. Change the element spacing d within the constraint range to obtain anthoer maximum value SLLmax. If the maximum value reduces, the element spacings will continue to change in this direction, otherwise the other direction will be chosen.

Repeat the above steps until SLLmax remains the same for multiple times or iterations reaches the allowable

maximum number.

To show the effectiveness and robustness of the proposed method, the comparisons with the UWB array and a uniformly spaced array are presented here. The uniformly spaced array has the same number of element and aperture size as the UWB array. The optimized element locations and uniformly element locations are illustrated in Fig. 1. The minimum spacing of the optimized array is $0.5043\lambda_L$, and the aperture size is $33.3\lambda_L$. The element spacing of the uniformly spaced linear arrays is $0.6656\lambda_L$. Figure 2 shows that the maximum SLL of the optimized array scanned patterns is -11.4 dB. However, the maximum SLL of the uniformly spaced array scanned patterns is 0 dB. We can see that compared to the uniformly spaced array, the proposed UWB array can significantly reduce the maximum SLL while maintaining almost the same array aperture and element numbers.
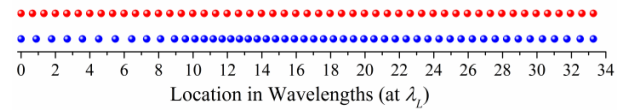

Fig. 1. Element locations of the uniformly spaced array and the optimized UWB array.
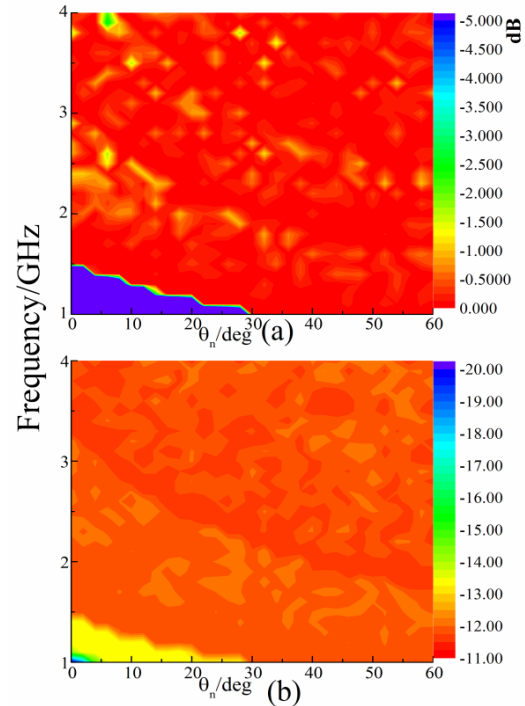

Fig. 2. The peak sidelobe levels of (a) the uniformly spaced array, and (b) the optimized UWB array in the frequency band, with steered from 0° to 60°.

III. POLARIZATION RECONGFIGURABLE TECHNOLOGY

The sequential rotation scheme was introduced by Huang in 1986 [18] to increase the axial ratio bandwidth of the circular polarization array. When arranging linearly polarized elements as shown in Fig. 3 (a), two equal orthogonal electric fields will be generated at broadside. And then, the circular polarization can be obtained with the phase excitations in 0°, 90°, 180°, 270°. Inspired by the above techniques, a novel polarization reconfigurable technique is proposed. For an array arranged as Fig. 3 (a), the four polarization (+45° LP, -45° LP, RHCP, and LHCP) can be obtained at broadside with unique phase arrangement as in Table 1 (Assuming that the co-polarized of the element is consistent with the arrow direction).
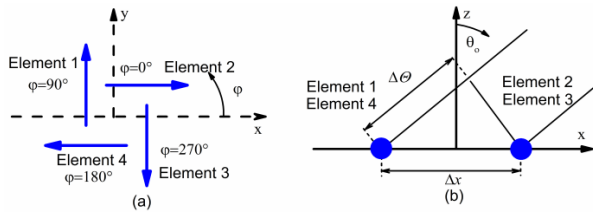

Fig. 3. (a) 2×2 array with elements in 0°, 90°, 180°, 270° directions. (b) Its spatial phase delay.

Table 1: The phase arrangements for four polarizations

	+45° LP	-45° LP	RHCP	LHCP
Element 1	0°	0°	0°	0°
Element 2	0°	180°	90°	270°
Element 3	180°	180°	180°	180°
Element 4	180°	0°	270°	90°

However, the approach is not suitable for scanning arrays. When the beam is steered away from the broadside, the polarization characteristics will severely degrade. One reason is the differences between the E-plane and H-plane patterns of linearly polarized elements. The other is that the spatial phase delay disturbs the required phase differences. The practical problem can be solved by compensating for the amplitudes and phases of the individual element [19]. We will illustrate the necessary procedure using a 2×2 array arranged as Fig. 3 (a). All the cases we discussed as followed are in $\varphi=0°$ plane.

Suppose the polarization reconfigurability in the θ_o direction is needed, two equal orthogonal electric fields would be required in the direction of θ_o. However, the differences between the two principal patterns of linearly polarized elements contribute to two orthogonal electric fields are unequal in the direction of θ_o. The basic idea of amplitude compensation is to pre-simulate each element patterns in the array. From the simulated patterns, the required amplitude correction values can be calculated.

$E_{1\theta}(\theta_o)$ and $E_{1\varphi}(\theta_o)$ are the θ-component and φ-component due to Element 1 for the direction of θ_o in $\varphi=0°$ plane, respectively. A similar explanation holds for the other field components. They are obtained by pre-simulating. $E_\theta(\theta_o)$ and $E_\varphi(\theta_o)$ represent the θ- and φ-components of the total electric field in the direction of θ_o, and can be expressed in (7) and (8). To obtain two equal orthogonal electric fields, a_j is introduced here, which represents the amplitude excitation of Element j:

$$E_\theta(\theta_o) = a_1 E_{1\theta}(\theta_o) + a_2 E_{2\theta}(\theta_o) + a_3 E_{3\theta}(\theta_o) + a_4 E_{4\theta}(\theta_o), \quad (7)$$

$$E_\varphi(\theta_o) = a_1 E_{1\varphi}(\theta_o) + a_2 E_{2\varphi}(\theta_o) + a_3 E_{3\varphi}(\theta_o) + a_4 E_{4\varphi}(\theta_o). \quad (8)$$

Set $a_1=a_3$ and $a_2=a_4$, and the amplitudes will be obtained as shown in (9) by solving $E_\theta(\theta_o)=E_\varphi(\theta_o)$:

$$\frac{a_2}{a_1} = \frac{\left[E_{1\theta}(\theta_o)+E_{3\theta}(\theta_o)\right] - \left[E_{1\varphi}(\theta_o)+E_{3\varphi}(\theta_o)\right]}{\left[E_{2\varphi}(\theta_o)+E_{4\varphi}(\theta_o)\right] - \left[E_{2\theta}(\theta_o)+E_{4\theta}(\theta_o)\right]}. \quad (9)$$

In addition, the spatial phase delay would disturb the required phase differential, and contribute to the poor polarization quality in the direction of θ_o as shown in Fig. 3 (b). The space phase compensation value required for Element 2 and Element 3 can be expressed as:

$$\Delta\Theta = -\beta\Delta x \sin\theta_o, \quad (10)$$

where Δx is the spacing between the two elements. For a large scanning array consisting of 2×2 sequential rotation subarray, the amplitude compensation values and phase arrangements required for polarization of the element are the same in different 2×2 subarray. However, the spatial phase delay compensation values vary from the locations of element in $\varphi=0°$ plane.

IV. THE DESIGN OF A RECONFIGURABLE ANTENNA ARRAY AND SIMULATED VALIDATIONS

An aperiodic array consisting of linearly polarized elements is placed on x-y plane as Fig. 4. The ideal dipoles are used to provide linearly polarized elements. The element positions in the direction of x-aixs are derived from the optimization results in Section II. Thus, the antenna array will have the ability to accurately control the sidelobe over a 4:1 bandwidth. The element spacing in the direction of y-axis is $\lambda_L/2$, where λ_L is the wavelength at the lowest frequency.
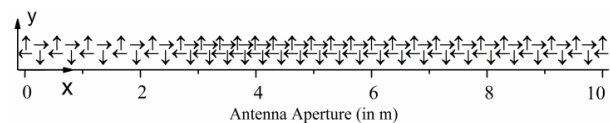

Fig. 4. The structure of the designed antenna.

According to (9), the amplitude compensation values of the ideal dipoles can be calculated, and the values are the same in different subarray as:

$$\frac{a_2}{a_1} = \frac{a_4}{a_3} = \frac{1}{\cos\theta_o} . \quad (11)$$

The phase excitation of the element consists of two parts, one is the space phase delay, and the other is the phase differential required by four polarizations. It is worth noting that the phase arrangements required for four polarizations are the same in different subarray, and it has been shown in Table 1. The space phase delay compensation values are $-\beta x_n \sin\theta_o$, where x_n is the locations of element in the direction of x-axis.

Figure 5 (a) shows that the patterns of the designed reconfigurable array antenna steered to 15°, 30°, 45°, and 55° with +45° LP, -45° LP, RHCP, and LHCP at 1 GHz. Figure 5 (b) shows that the patterns of the array antenna steered to 0°, 20°, 40°, and 60° with +45° LP, -45° LP, RHCP, and LHCP at 4 GHz. Figure 6 shows axial ratios of the circular polarized scanned patterns.

From Figs. 5-6, it can be observed that the four polarizations can be obtained at different scanning angles. The simulation results show that the method can be used to design the UWB, wide-angle scanning, and polarization reconfigurable antenna arrays. When considered a more realistic wideband linearly polarized element, we need to account for variations element pattern over bandwidth. A more excellent polarization performance will be obtained by calculating the element amplitude compensation values at different operating frequencies.
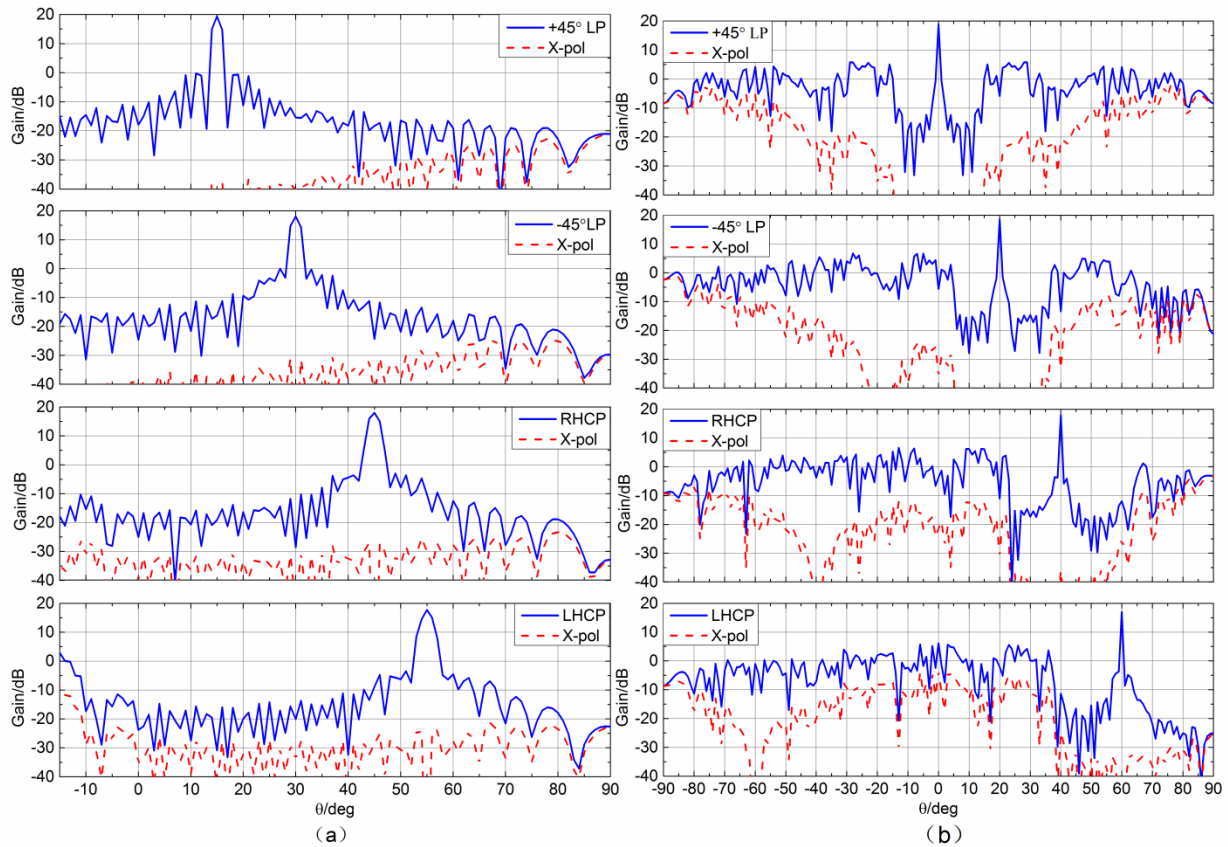

Fig. 5. (a) The radiation pattern at 1 GHz. The main beam is steered to 15° with +45° LP, 30° with -45° LP, 45° with RHCP, and 55° with LHCP. (b) The radiation pattern at 4 GHz. The main beam is steered to 0° with +45° LP, 20° with -45° LP, 40° with RHCP, 60° with LHCP.
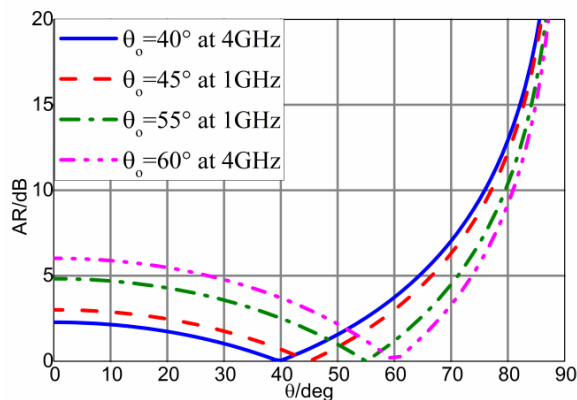
Fig. 6. Axial ratios for the circular polarized scanning.

V. CONCLUSION

A beam-scanning UWB array consisting of linearly polarized elements is proposed for polarization reconfiguration. Through optimizing multiple radiation patterns simultaneously, the UWB array synthesis approach can control the sidelobe level in the ultrawide frequency band. An iterative convex optimization strategy is used to successively optimize the element spacing for SLL reduction. The sequential rotation and excitation compensation (SR-EC) technique provides polarization reconfigurable electrical scanning ability for UWB aperiodic arrays. This paper presents an effective approach of designing multifunctional arrays.

ACKNOWLEDGMENT

REFERENCES

[1] B. Wang, S. Yang, Y. Chen, S. Qu, and J. Hu, "Low cross-polarization ultrawideband tightly coupled balanced antipodal dipole array," *IEEE Trans. Antennas Propag.*, vol. 68, no. 6, pp. 4479-4488, June 2020.

[2] W. F. Moulder, K. Sertel, and J. L. Volakis, "Superstrate-enhanced ultrawideband tightly coupled array with resistive FSS," *IEEE Trans. Antennas Propag.*, vol. 60, no. 9, pp. 4166-4172, Sep. 2012.

[3] E. Yetisir, N. Ghalichechian, and J. L. Volakis, "Ultrawideband array with 70° scanning using FSS superstrate," *IEEE Trans. Antennas Propag.*, vol. 64, no. 10, pp. 4256-4265, Oct. 2016.

[4] H. Zhang, S. Yang, S.-W. Xiao, Y. Chen, S.-W. Qu, and J. Hu, "Ultrawideband phased antenna arrays based on tightly coupled open folded dipoles," *IEEE Antennas Wireless Propag. Lett.*, vol. 18, no. 2, pp. 378-382, Feb. 2019.

[5] R. L. Haupt, "Genetic algorithm applications for phased arrays," *Applied Computational Electromagnetics Society Journal*, vol. 21, no. 3, pp. 1054-4887, Nov. 2006.

[6] M. H. Rahmani and A. Pirhadi, "Optimum design of conformal array antenna with a shaped radiation pattern and wideband feeding network," *Applied Computational Electromagnetics Society Journal*, vol. 29, no. 1, pp. 1054-4887, Jan. 2014.

[7] W. Shi, Y. Li, and S. A. Vorobyov, "Low mutual coupling sparse array design using ULA fitting," in *Proc. ICASSP. IEEE*, pp. 4610-4614, May 2021.

[8] W. Shi, S. A. Vorobyov, and Y. Li "ULA fitting for sparse array design," arXiv e-prints, arXiv: 2102.02987, Feb. 2021.

[9] W. Shi, Y. Li, L. Zhao, and X. Liu, "Controllable sparse antenna array for adaptive beamforming," *IEEE Access*, vol. 7, pp. 6412-6423, Jan. 2019.

[10] Y. Liu, Y. Yang, F. Han, Q. H. Liu, and Y. J. Guo, "Improved beam-scannable ultra-wideband sparse antenna arrays by iterative convex optimization based on raised power series representation," *IEEE Antennas Wireless Propag. Lett.*, vol. 68, no. 7, pp. 1-1, 2020.

[11] M. D. Gregory and D. H. Werner, "Ultrawideband aperiodic antenna arrays based on optimized raised power series representations," *IEEE Trans. Antennas Propag.*, vol. 58, no. 3, pp. 756-764, Mar. 2010.

[12] Y. J. Sung, T. U. Jang, and Y. S. Kim, "A reconfigurable microstrip antenna for switchable polarization," *IEEE Antennas Wireless Propag. Lett.*, vol. 14, no. 11, pp. 534-536, Nov. 2004.

[13] C. Wenquan, Z. Bangning, L. Aijun, Y. Tongbin, G. Daosheng, and P. Kegang, "A reconfigurable microstrip antenna with radiation pattern selectivity and polarization diversity," *IEEE Antennas Wireless Propag. Lett.*, vol. 11, pp. 453-456, Feb. 2012.

[14] N. N.-T. Muhammad Ikram and Amin Abbosh, "A simple single-layered continuous frequency and polarization-reconfigurable patch antenna array," *IEEE Trans. Antennas Propag.*, vol. 10, no. 1109, pp. 1-6, 2019.

[15] Y. Fan, R. Li, and Y. Cui, "Development of polarisation reconfigurable omnidirectional antennas using crossed dipoles," *IET Microw. Antenna P*, vol. 13, no. 4, pp. 485-491, Nov. 2019.

[16] J.-S. Row and Y.-H. Wei, "Wideband reconfigurable crossed-dipole antenna with quad-polarization diversity," *IEEE Trans. Antennas Propag.*, vol. 66, no. 4, pp. 2090-2094, Apr. 2018.

[17] B. Babakhani, S. K. Sharma, and N. R. Labadie, "A frequency agile microstrip patch phased array antenna with polarization reconfiguration," *IEEE Trans. Antennas Propag.*, vol. 64, no. 10, pp. 4316-4327, Oct. 2016.

[18] J. Huang, "A technique for an array to generate circular polarization with linearly polarized elements," *IEEE Trans. Antennas Propag*., vol. 34, no. 9, pp. 1113-1124, Sep. 1986.

[19] A. B. Smolders and U. Johannsen, "Axial ratio enhancement for circularly-polarized millimeter-wave phased-arrays using a sequential rotation technique," *IEEE Trans. Antennas Propag*., vol. 59, no. 9, pp. 3465-3469, Sep. 2011.